IJME

Int. J. of Applied Mechanics and Engineering, 2024, vol.29, No.2, pp.79-89
DOI: 10.59441/ijame/186956

PROCESS PARAMETERS INFLUENCE THE MECHANICAL PROPERTIES AND NUGGET DIAMETER OF AISI 316 STAINLESS STEEL DURING RESISTANCE SPOT WELDING

Mahmood Mohammed Hamzah
College of Engineering, Al-Iraqia University, Baghdad, IRAQ

Osamah Sabah Barrak*
Institute of Technology - Baghdad, Middle Technical University, Baghdad, IRAQ
E-mail: usamah.barrak@yahoo.com

Isam Tareq Abdullah
Engineering Technical College - Baghdad, Middle Technical University, Baghdad, IRAQ

Aws Abdulillah Hussein
College of Engineering, Al-Iraqia University, Baghdad, IRAQ

Sabah Khammass Hussein
Engineering Technical College - Baghdad, Middle Technical University, Baghdad, IRAQ

Resistance spot welding (RSW) is an important fusion welding process used in many applications, including storage tanks, pipes, and medical tools. For this, should be improved the joints and developing the process parameters and through this research will be discussed the results and concept development. Herein, *1 mm*-thick AISI 316 austenitic stainless steel was welded by RSW, and the effect of the welding process parameters, such as "welding current, pulses, squeeze time, and welding time", on the mechanical properties, nugget diameter (ND), and microstructure of AISI 316 were investigated. As a result, there was a direct relationship between shear-tensile force and ND. The maximum shear-tensile force (*12.5 kN*) was obtained using *7500 A*, *3* pulses, *1.8 s* squeeze time, and 1 s welding time. The ND was maximized using *7500 A*, *3* pulses, *1.6 s* squeeze time, and *0.8 s* welding time. The DOE analysis gives an indication about the relation between the parameters and ND on the hand and the parameters and shear strength on the other hand. The microstructure was investigated by optical microscopy, revealing the presence of martensitic, widmanstatten austenite, and ferrite structures.

Keywords: nugget diameter; resistance spot welding; welding parameters; pulse; design of experiment.

1. Introduction

The Resistance Spot Welding process is one of the important welding methods, and so it was utilized as a joining process in stainless steel welding which had a thin thickness for manufacturing structures, particularly in the lightweight industries, building ships, and automotive. Automobiles generally require more than *3000* welds performed by resistance spot welding (RSW) [1-3], which is the most suitable technique for rapidly joining metal sheets and plates. Notably, the common applications of RSW are railway vehicles, appliances, buses, truck trailers, recreational vehicles, and office furniture. RSW is also applied in space and aeronautical applications [4-6] and can be used to weld similar and dissimilar metals [7-9]. For example, an aluminium joint can be joined to steel by RSW [10-12].

* To whom correspondence should be addressed

The RSW process involves multiple physical interactions, including electrical, mechanical, metallurgical, and thermal phenomena. The major process parameters are "welding current, pressure, squeeze time, and welding time". The weld quality is mainly influenced by the welding current, welding time, and electrode force. Multiple-solidification welding schedules and multi-ring domed electrodes are used to obtain high-quality weld nuggets with high joint strength [13]. Moreover, the design of experiment (DOE) approach can be used to determine the effects of RSW parameters on the properties of welded joints. The welding current is the most influential factor on the molten metal pool and the heat-affected zone (HAZ). Changes in "sheet thickness and welding time" also contribute to the weld properties, but the effects of the other parameters were less important [14].

In this study, the influence of the microstructure of metallic sheets on the mechanical properties of the RSW was evaluated, considering that homogeneous spot welds usually provide high shear-tensile strength [15]. The size and shape of the weld nuggets (WN) are related to the quality and strength of the RSW welds. In the RSW process, heat generation and nugget size are directly correlated. The heat generated through welding and the resulting shape and size of the WN are primarily determined by the contact resistances at the faying surface between workpieces, as well as the "welding current, welding time, and sheet thickness" [16, 17]. Welding current and time can be raised to make the nuggets bigger. However, an increase in welding energy may result in significant surface indentations and weld spatter because the resistance heat typically concentrates in the nugget's centre. Because of the increased stress concentration, the nugget strength may be reduced, and the welding process may become unstable [18-22]. These process parameters must be optimised to acquire the maximum WN size and joint force.

In contrast, the temperature created at the sheet/electrode interface and subsequent weld oxidation has received less attention. The oxidation of stainless steel is a well-known result of chromium depletion in the material, thus affecting its corrosion resistance properties [23]. The mechanical properties are improved by using the acceptable current range and suitable conditions to increase the spot weld size [24]. In the present study, Minitab was utilised to analyse the effects of the technique parameters on the joint properties, considering that the surface treatment can significantly affect the shear strength [25, 26]. RSW was conducted to weld alloy materials according to the "AWS/ANSI C1.1M/C1.1:2012 standard", while accounting for the "welding current, pulses, squeezing time, and welding time" [27].

Specifically, the effects of the RSW method parameters on the mechanical properties and size of weld nuggets were studied, using AISI 316 stainless steel. The results were analysed using the design of the experiment method (DOE) to evaluate the influence of each parameter on the nugget diameter (ND) and mechanical properties. These results can be employed to optimise the RSW parameters for joining AISI 316. DOE is a structured approach for collecting data and making discoveries.

2. Experimental procedure

2.1. Material and specimen

The AISI 316 alloy was used because of the higher importance of its applications with *1 mm* thickness welded employing the RSW process, as illustrated in Fig.1, which indicates the dimensions of the welded samples and welding region. The mechanical properties and chemical composition of the AISI 316 are displayed in Tabs 1 and 2, respectively.

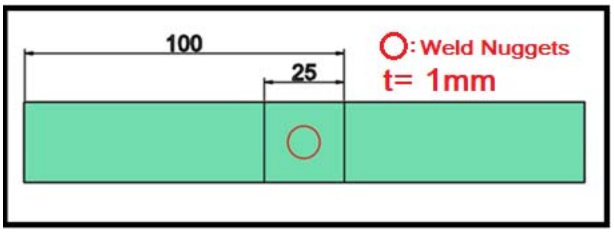

Fig.1. Schematic of welded sample.

The parameters employed for welding the samples are indicated in Tab.3. The samples were joined by RSW based on the parameters listed in Tab.3, and representative results are shown in Fig.2. All the parameters within the acceptance criteria of the resistance spot welding.

Table 1. Mechanical properties AISI 316.

Material Property	Yield strength σ_y, (*MPa*)	Tensile strength σ_u, (*MPa*)	Elongation (%)	Hardness Brinell HB
AISI 316	*285*	*636*	*34*	*198*

Table 2. The chemical composition of AISI 316.

Element wt%	AISI 316
C	*0.07*
Cr	*17.3*
Ni	*11.4*
Mo	*2.62*
Mn	*1.19*
P	*0.025*
Si	*0.52*
S	*0.02*
N	*0.08*
Fe	Bal.

Table 3. Process parameters used for joining AISI 316.

No.	Welding current (*A*)	Sq. time (*sc.*)	welding time (*sc.*)	Pulse
1	*4500*	*1.2*	*0.6*	*1*
2	*4500*	*1.6*	*0.8*	*2*
3	*4500*	*1.8*	*1*	*3*
4	*6000*	*1.2*	*0.8*	*3*
5	*6000*	*1.6*	*1*	*1*
6	*6000*	*1.8*	*0.6*	*2*
7	*7500*	*1.2*	*1*	*2*
8	*7500*	*1.6*	*0.6*	*3*
9	*7500*	*1.8*	*0.8*	*1*

2.2. Shear-tensile force test

Shear-tensile force tests were performed at room temperature with a maximum load of *50 kN* and a crosshead velocity of *10 mm/s*. The spot-welded behaviour of AISI 316 under static load was assessed to determine the force and ND after failure.

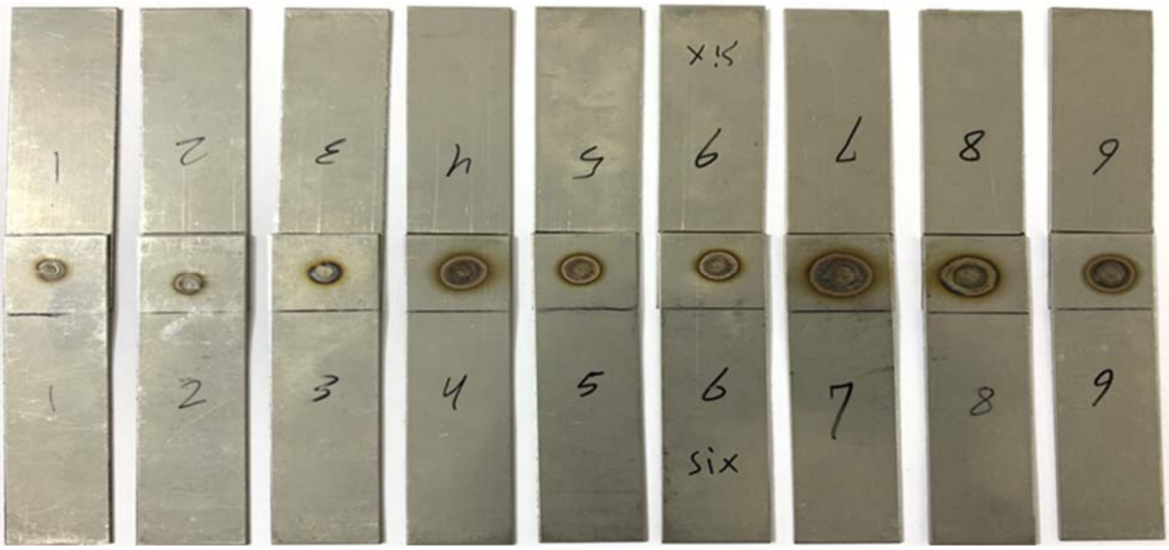

Fig.2. The welded samples.

2.3. Microstructure test

The sample was cut across the transverse direction of the welding joint, and various preparation procedures “(mounting, grinding, polishing, and etching, respectively)” were performed to acquire smooth and mirror-like surfaces.

Mounting: The metal sample is mounted by placing it in a mold and then filling the mold by a suitable material that embeds the metal sample and holds it firmly.

Grinding: this process removes cutting marks and cleans the specimen surface, The principle of this process is depends on the fact that it is abrasive particles in succession finer grain sizes are utilized to remove materials from the surface of the sample Until getting the desired result.

Polishing: The purpose of this process is to ensure that the sample structure is made visible with a superficial finish that didn’t disturb the examination. This is typically done in two or three steps using suitable cloths of polishing and progressively finer abrasives.

Etching: A chemical technique process is utilized to highlight materials features at microscopic levels. An optical microscope was employed to inspect the morphology and microstructure.

3. Results and discussion

In this research the results are discussed with the other researchers and with the aid of DOE improved the results. Many applications can use these results in manufacturing and industries.

3.1. Shear-tensile force

The shear-tensile specimens exhibited button pull-out, making it possible to estimate the ND. It also quantified the shear-tensile force of the welded joints, providing information about the spot weld failure mechanisms and joint quality.

Figure 3 displays the welded samples after the shear test, revealing the fracture surfaces of the RSW joints, including peeling fracture and shearing-off fracture, with and without deformation [28].

The shearing-off fracture without deformation: provide an indication of low-quality RSW process joints.

For shearing-off fracture with deformation: the adhesive forces between the two samples of steel plate were higher than that for shearing-off fracture without deformation.

For peeling fracture: the nucleated cracks around the RSW process joints, and propagated along the RSW joints edge with increasing displacement. The RSW process lab joints with peeling fracture had higher shearing tensile strength and deformation than those with shearing-off fracture.

The ultimate shear-tensile strength indicates the highest fracture resistance of the welded joint. Figure 4 indicates the shear-tensile force results. The maximum shear-tensile force was *12.5 kN* (sample No.7), the minimum was *3.7 kN* (sample No.1), and the welding parameters of the sample are specified in Tab.3.

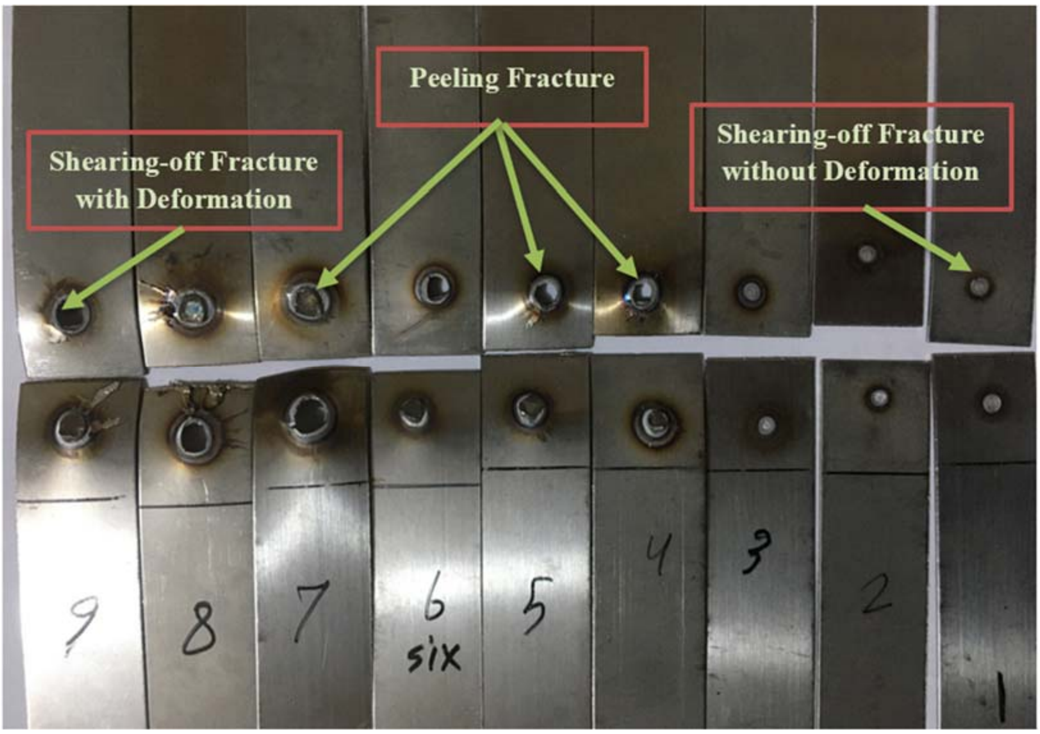

Fig.3. The samples after shear-tensile testing.

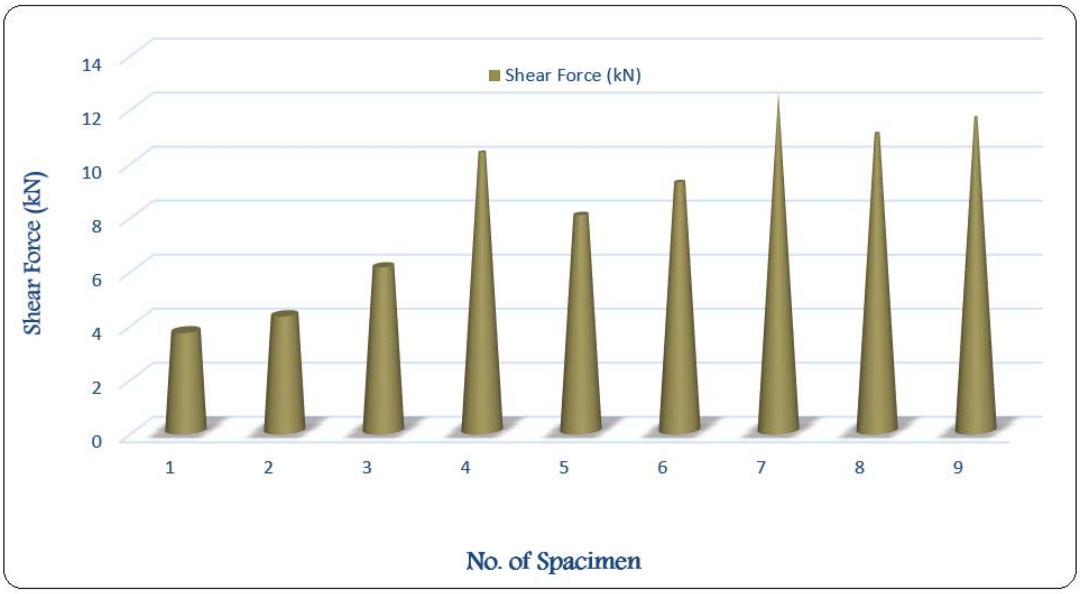

Fig. 4. Shear-tensile force

3.2. Design of experiment (DOE)

The shear-tensile force test results were analysed based on the DOE, which helps explain the effects of various parameters on the mechanical properties and ND.

Figure 5 indicates the effects of welding parameters on shear-tensile force:

- The shear-tensile force increases as the welding current increases.
  With the increasing welding current for the RSW process, the amount of melting of the base metal will be increased gradually, which will increase the weld nugget width. Thus, the strength of bonding of the RSW joint increased, and the tensile shear force increased as a result.
- The shear-tensile force increases as the pulse increases.
  The increase in pulse will enlarge the connection joint area between the two samples, and as a result, will increase the joint strength.
- Squeeze time has a variable effect on shear-tensile force. The shear-tensile force is higher at *1.2 s* than at *1.6 s* and then increases to the maximum value at *1.8 s*.
- The shear-tensile force continuously increases as the welding time increases.

Figure 6 displays the effects of welding parameters on the ND:

- The ND increases as the welding current increases.
- Increasing the pulse also increases the ND.
- Squeeze time has a variable effect on ND, which increases at *1.2-1.6 s* and then decreases at *1.8 s*.
- Welding time has a variable effect on ND, which increases at *0.6-0.8* s and then decreases at *1 s*.

Improving the weld nugget gives a good tensile strength [13, 18]. The size and shape of the weld nuggets controlled the quality and strength of the joints [16, 17].

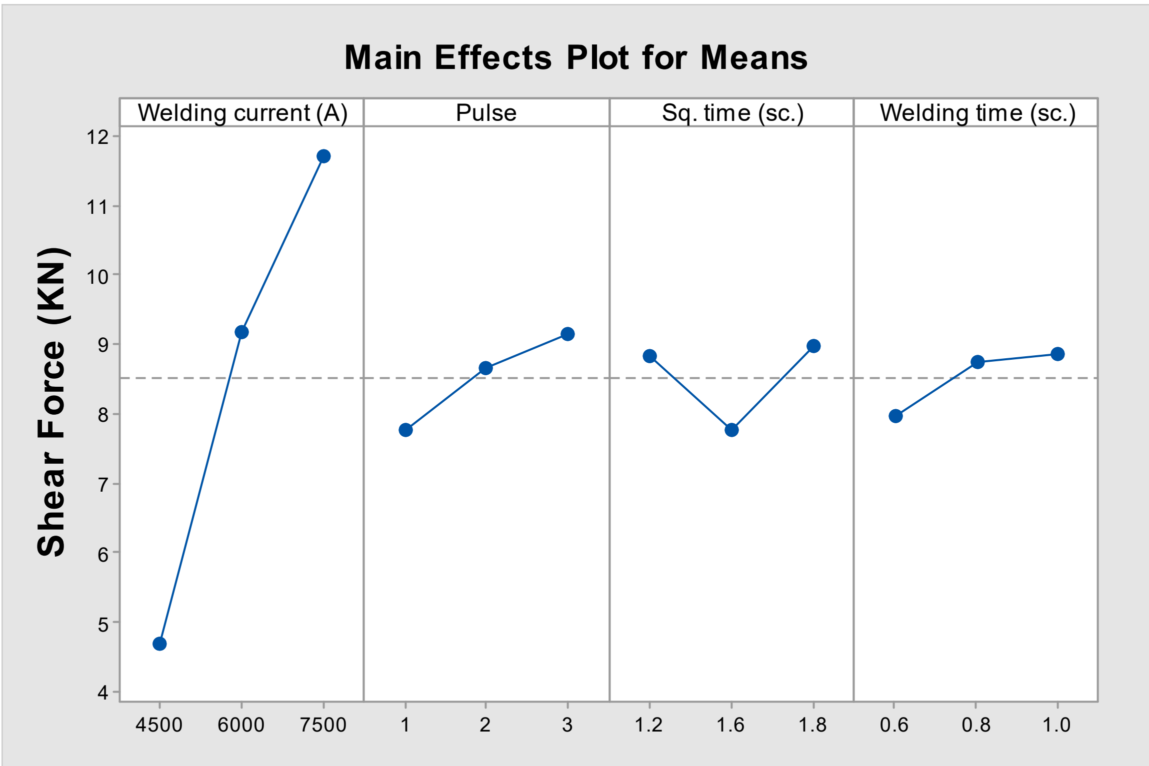

Fig.5. Mean effects of parameters on shear-tensile force.

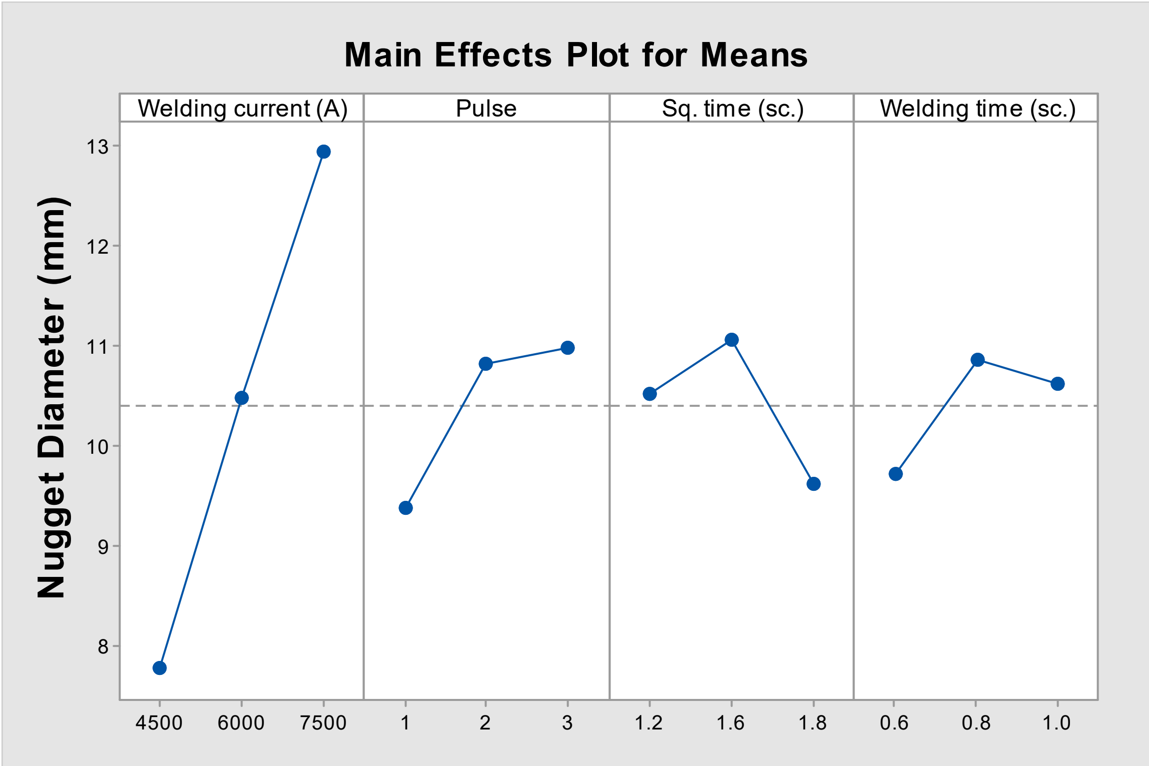

Fig.6. Means effects of parameters on ND.

3.3. Relation between the shear-tensile force and the nugget diameter (ND)

Figure 7 shows the NDs obtained after performing the shear-tensile test. The lowest ND was *6.2 mm*, and the largest ND was *13.7 mm*, which occurred for samples No.1 and 7, respectively. The most widely employed metric for evaluating the quality of a weld is the ND. The amount of energy that the joint can absorb before failing, and thus its strength, is often inferred from the measured ND [29].

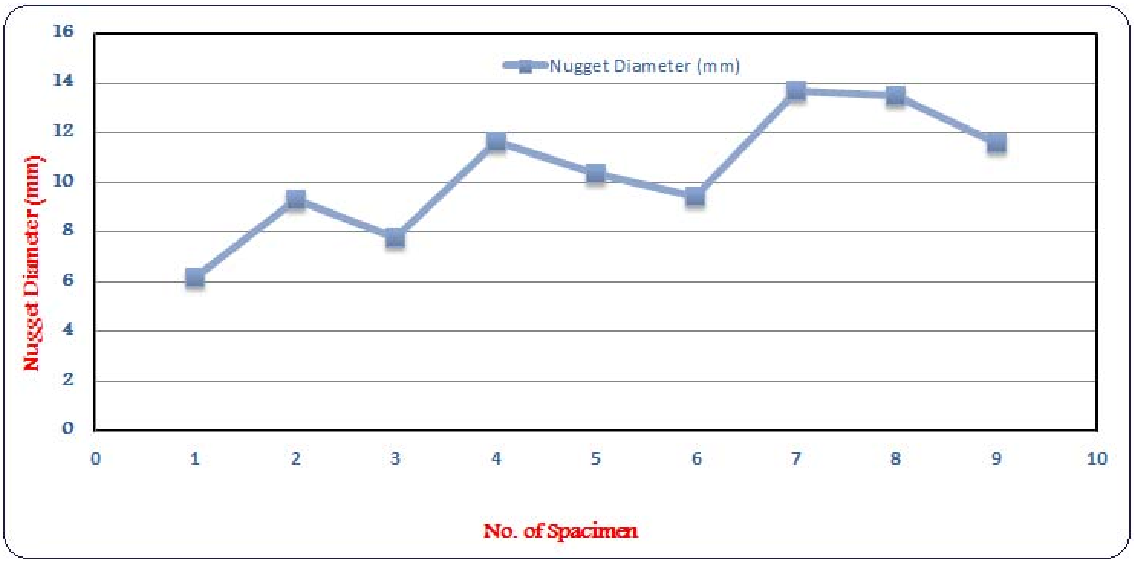

Fig.7. NDs of the samples after shear-tensile force testing.

The relation between the shear-tensile force and the ND is shown in Fig.8. The shear-tensile force increased when the ND increased from *6.2* to *11.65 mm*. However, it suddenly decreased at *10.35 mm* and then recovered, reaching the maximum shear-tensile force at the maximum ND. Direct correlations were found between ND and the tensile-shear force for AISI 316. A smaller spot diameter indicates a weaker joint, but a larger spot diameter and larger ND can provide a sufficient joint quality [29].

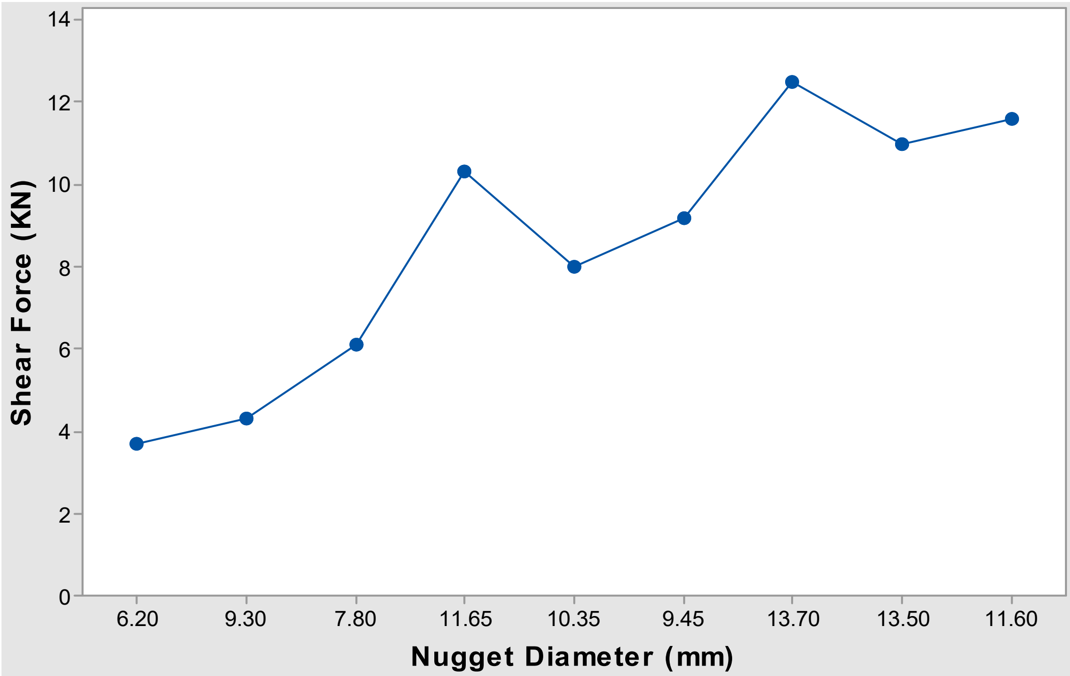

Fig.8. The relationship between shear-tensile force and ND.

3.4. Microstructure test.

Figures 9 and 10 shows the microstructure of the welding zone, base metal, and HAZ.

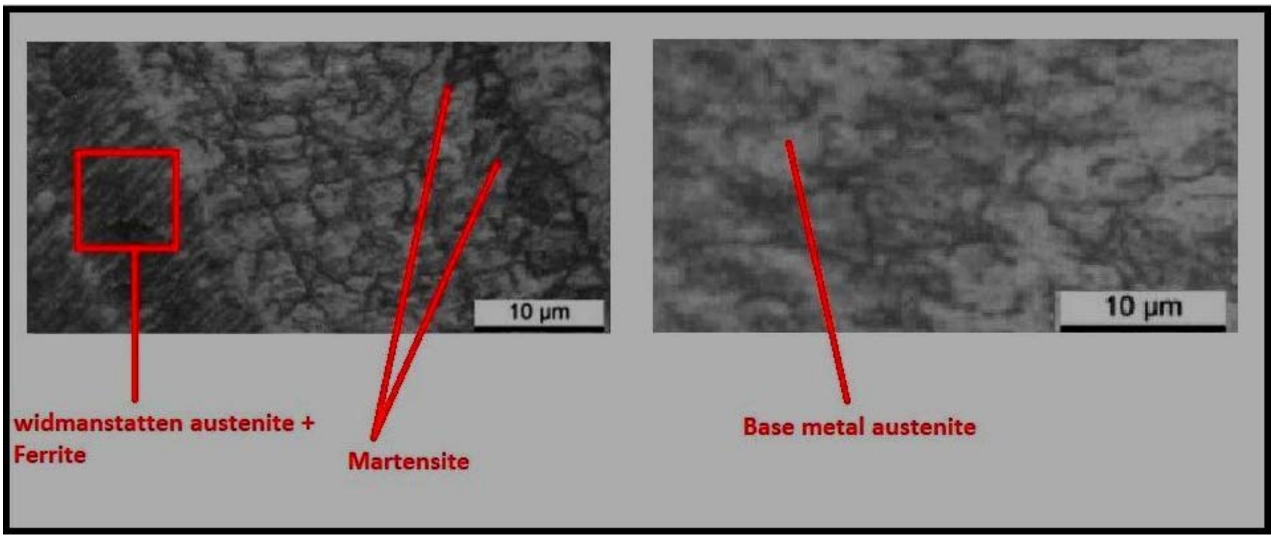

Fig.9. The microstructure of the AISI 316 welding zone.

The solid-liquid phase transformation was observed in the welding zone. In the welding zone, columnar grains formed in the direction of the compression force imposed by the electrode. The presence of martensitic, widmanstatten austenite, and ferrite structures was confirmed, as shown in Fig.6, because the fast cooling rate of the molten metal. Martensitic and widmanstatten austenite structures form in hypoeutectic stainless steel during fast cooling and there is no preheat or post heat treatment. The HAZ is indicated in Fig.7, where no phase transformation occurs, just grain growth [30]. For improving the microstructure should be preheating and post-heat treatment for the weld nugget to achieve better microstructure.

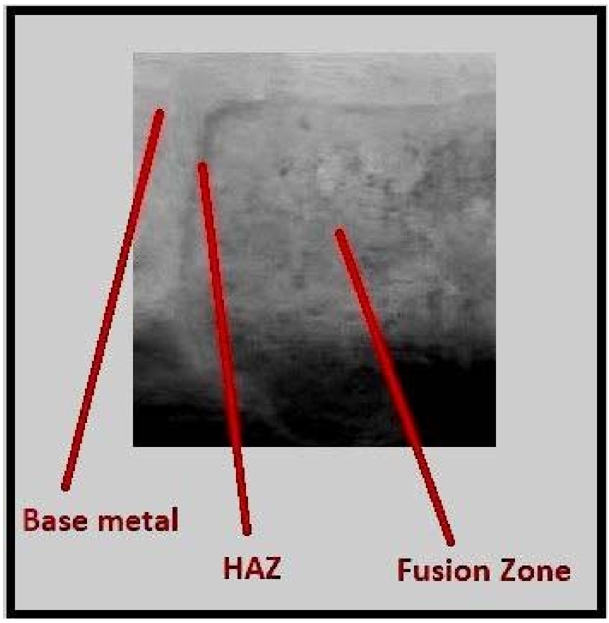

Fig.10. Optical images of the base metal, HAZ, and fusion zone.

4. Conclusion

RSW and the effects of "welding current, pulses, squeeze time, and welding time" on the shear-tensile force, ND, and microstructure of AISI 316 were investigated in this study. The results demonstrated that the welding current and pulse significantly affected the shear-tensile force because they are directly associated with heat generation during welding. Furthermore, an increase in ND influenced the shear-tensile force of the welded joint, which contained martensitic, widmanstatten austenite, and ferrite structures. In the future many problems can be studied like; the improvement of microstructure by preheating and post-heating, using other parameters and its effect on the weld nugget, …etc.

This research solved many problems which face manufacturing and contributed to improving the industries which deal with the RSW of stainless steel.

Acknowledgements

We want to thank the Department of Technical Applied Mechanical Engineering, Engineering Technical College - Baghdad, Middle Technical University, Baghdad, Iraq, and the department's teaching staff for their assistance.

Nomenclature

RSW – Resistance Spot Welding
AISI – American Iron and Steel Institute

ND – Nugget Diameter
DOE – Design of Experiment
HAZ – Heat-Affected Zone
WN – Weld Nuggets

References

[1] Zhou K. and Yao P. (2019): *Overview of recent advances of process analysis and quality control in resistance spot welding*.– Mechanical Systems and Signal Processing, vol.124, pp.170-198, https://doi.org/10.1016/j.ymssp.2019.01.041.

[2] Hassoni S.M., Barrak O.S., Ismail M.I. and Hussein S.K. (2022): *Effect of welding parameters of resistance spot welding on mechanical properties and corrosion resistance of 316L*.– Materials Research, vol.25, https://doi.org/10.1590/1980-5373-MR-2021-0117.

[3] Al-Mukhtar A.M. (2016): *Review of resistance spot welding sheets: processes and failure mode*.– In: Advanced Engineering Forum, Trans. Tech. Publ, Ltd, pp.31-57, https://doi.org/10.4028/www.scientific.net/AEF.17.31.

[4] Osamah Sabah Barrak, Osamah Fattah Taresh, Mahmood Mohammed Hamzah and Rusul Ahmed Shakir (2023): *An investigation of joining polyamide (PA) to* Stainless Steel *AISI 316L by hot press process*.– Journal of Techniques, vol.5, No.1, pp.114-121, https://doi.org/10.51173/jt.v5i1.1280.

[5] Pouranvari M. and Marashi S.P.H. (2013): *Critical review of automotive steels spot welding: process, structure and properties*.– Science and Technology of Welding and Joining, vol.18, No.5, pp.361-403, https://doi.org/10.1179/1362171813Y.0000000120.

[6] Barrak O.S, Sar M.H, Saad M.L, Hussein A.K. and Hussein S.K. (2019): *Using brass foil interlayer to improve the resistance spot welding AA5451 with apply taguchi method*.– J. Mech. Eng. Res. Dev., vol.42, No.3, pp.120-124.

[7] Pouranvari M., Alizadeh S.H.M. and Marashi S.P.H. (2015): *Welding metallurgy of stainless steels during resistance spot welding Part I: fusion zone*.– Science and Technology of Welding and Joining, vol.20, No.6, pp.502-511, https://doi.org/10.1179/1362171815Y.0000000015.

[8] Husain I.M., Saad M.L., Barrak O.S., Hussain S.K. and Hamzah M.M. (2021): *Shear force analysis of resistance spot welding of similar and dissimilar material: copper and carbon steel*.– Mater. Sci. Eng., vol.1105, No.1, pp.012055.

[9] Akkaş N. (2017): *Welding time effect on tensile-shear loading in resistance spot welding of SPA-H weathering steel sheets used in railway vehicles*.– Acta Physica Polonica A, vol.131, No.1, pp.52-54, http://doi.org/10.12693/APhysPolA.131.52.

[10] Barrak, O.S., Hamzah M.M. and Hussein S.H. (2022): *Friction stir spot welding of pure copper (c11000) with pre-holed threaded aluminum alloys (AA5052)*.– Journal of Applied Science and Engineering, vol.26, No.8, pp.1103-1110, https://doi.org/10.6180/jase.202308_26(8).0006.

[11] Jagadeesha T. (2017): *Experimental studies in weld nugget strength of resistance spot-welded 316L austenitic stainless steel sheet*.– The International Journal of Advanced Manufacturing Technology, vol.93, pp.505-513, https://doi.org/10.1007/s00170-017-0517-5.

[12] Sigler D.R., Carlson B.E. and Karagoulis M.J. (2019): *Multi-stage resistance spot welding method for workpiece stack-up having adjacent steel and aluminum workpieces*.– U.S. Patent No., vol.10, No.245, pp.675.

[13] Kang J., Shi L., Shalchi-Amirkhiz B., Sigler D., Haselhuhn A. and Carlson B. (2020): *Microstructure and shear strength of novel aluminum to steel resistance spot welds*.– Welding Journal, vol.99, pp.67-74, https://doi.org/10.29391/2020.99.007.

[14] Eshraghi M., Tschopp M.A., Zaeem M.A. and Felicelli S.D. (2014): *Effect of resistance spot welding parameters on weld pool properties in a DP600 dual-phase steel: A parametric study using thermomechanically-coupled finite element analysis*.– Materials & Design (1980-2015), vol.56, pp.387-397, http://dx.doi.org/10.1016/j.matdes.2013.11.026.

[15] Essoussi H., Elmouhri S., Ettaqi S. and Essadiqi E. (2019): *Microstructure and mechanical performance of resistance spot welding of AISI 304 stainless steel and AISI 1000 series steel*.– Procedia Manufacturing, vol.32, pp.872-876, https://doi.org/10.1016/j.promfg.2019.02.296.

[16] Wahed S.N.A., Hussein S.K. and Al-Saadi M.H. (2022): *Disc forming by friction stir consolidation of AA2024 chips*.– Journal of Techniques, vol.4, No.1, pp.1-8, https://doi.org/10.51173/jt.v4i1.442.

[17] Eisazadeh Hamid, Hamedi Mohsen and Halvaee Ayob. (2010): *New parametric study of nugget size in resistance spot welding process using finite element method*.– Materials & Design, vol.31, No.1, pp.149-157, https://doi.org/10.1016/j.matdes.2009.06.042.

[18] Zhao D., Ren D., Song G., Zhao K., Liu L. and Zhang Z. (2020): *Comparison of mechanical properties and the nugget formation of composite ceramic-centered annular welding and traditional resistance spot welding*.– International Journal of Mechanical Sciences, vol.187, No.105933, https://doi.org/10.1016/j.ijmecsci.2020.105933.

[19] Ridha M.H., Saad M.L., Abdullah I.T., Barrak O.S., Hussein S.K. and Hussein A.K. (2022): *Joining of carbon steel AISI 1006 to aluminum alloy AA6061-T6 via friction spot joining technique*.– International Journal of Applied Mechanics and Engineering, vol.27, No.4, pp.1-12.

[20] Abdullah I.T. (2022): *Friction spot joining of aluminium alloy AA 5052 to pre-holed steel AISI 1006 by extrusion of aluminium into a rivet head die*.– Journal of Techniques, vol.4, No.2, pp.10-20, https://doi.org/10.51173/jt.v4i2.492.

[21] Barrak O.S., Saad M.L., Mezher M.T., Hussein S.K. and Hamzah M.M. (2020): *Joining of double pre-holed aluminum alloy AA6061-T6 to polyamide PA using hot press technique*.– IOP Conf. Series Mater. Sci. Eng., vol.881, No.1, pp.012062.

[22] Brauser S., Pepke L.A., Weber G. and Rethmeier M. (2020): *Deformation behaviour of spot-welded high strength steels for automotive applications*.– Mater. Sci. Eng., vol.527, No.26, pp.7099-7108, https://doi.org/10.1016/j.msea.2010.07.091.

[23] Bhat S.D., Vijeesh V., Acharya P. and Rao M. (2021): *Investigation of thin sheet stainless steel resistance spot welds: Effect of weld current on nugget failure and microstructure*.– Materials Today: Proceedings, vol.35, pp.361-365, https://doi.org/10.1016/j.matdes.2004.11.027.

[24] Cheon J.Y., Vijayan V., Murgun S., Park Y.D., Kim J.H., Yu J.Y. and Ji C. (2019): *Optimization of pulsed current in resistance spot welding of Zn-coated hot-stamped boron steels*.– Journal of Mechanical Science and Technology, vol.33, pp.1615-1621, https://doi.org/10.1007/s12206-019-0313-2.

[25] Mezher M.T., Barrak O.S. and Namer N.S.M. (2022). *Modelling and experimental study of dissimilar arc stud welding of AISI 304L to AISI 316L stainless steel*.– Int. Journal of Integrated Engineering, vol.14, No.6, pp.88-101.

[26] Hamzah M.M. and Hussein S.K. (2020): *Effect of surface pretreatment on hot press lap joining of high density polyethylene to stainless steel alloy AISI 304L*.– In: IOP Conference Series: Materials Science and Engineering. IOP Publishing, p.012058.

[27] American Welding Society (2012): *Recommended practices for resistance welding*.– American National Standards Institute, ANSI, AWS/ ANSI C1.1M/C1.1:2012.

[28] Chen L., Zhang Y., Xue X., Wang B., Yang J., Zhang Z. and Barber G.C. (2022): *Investigation on shearing strength of resistance spot-welded joints of dissimilar steel plates with varying welding current and time*.– Journal of Materials Research and Technology, vol.16, pp.1021-1028, https://doi.org/10.1016/j.jmrt.2021.12.079.

[29] Summerville C., Compston P. and Doolan M. (2019): *A comparison of resistance spot weld quality assessment techniques*.– Procedia Manufacturing, vol.29, pp.305-312.

[30] Khan M.I., Kuntz M.L., Biro E. and Zhou Y. (2008): *Microstructure and mechanical properties of resistance spot welded advanced high strength steels*.– Materials Transactions, vol.49, No.7, pp.1629-1637, https://doi.org/10.2320/matertrans.MRA2008031.

Received: February 6, 2024
Revised: April 9, 2024